Empirical analysis of the lane formation process in bidirectional pedestrian flow

Claudio Feliciani[1,*] and Katsuhiro Nishinari[2,3]

[1]*Department of Advanced Interdisciplinary Studies, Graduate School of Engineering, The University of Tokyo, 4-6-1 Komaba, Meguro-ku, Tokyo 153-8904, Japan*

[2]*Department of Aeronautics and Astronautics, Graduate School of Engineering, The University of Tokyo, 7-3-1 Hongo, Bunkyo-ku, Tokyo 113-8656, Japan*

[3]*Research Center for Advanced Science and Technology, The University of Tokyo, 4-6-1 Komaba, Meguro-ku, Tokyo 153-8904, Japan*

(Dated: May 7, 2019)

Abstract

This paper presents an experimental study on pedestrian bidirectional streams and the mechanisms leading to spontaneous lane formation by examining the flow formed by two groups of people walking toward each other in a mock corridor. Flow-ratio is changed by changing each group size while maintaining comparable total flow and density. By tracking the trajectories of each pedestrian and analyzing the data obtained, five different phases were recognized as contributing to the transition from unidirectional to bidirectional flow including the spontaneous creation and dissolution of lanes. It has been shown that a statistical treatment is required to understand the fundamental characteristics of pedestrian dynamics and some 2D quantities such as order parameter and rotation range were introduced to allow a more complete analysis. All the quantities observed showed a clear relationship with flow-ratio and helped distinguishing between the different characteristic phases of the experiment. Results show that balanced bidirectional flow becomes the most stable configuration after lanes are formed, but the lane creation process requires pedestrians to laterally move to a largest extent compared to low flow-ratio configurations. This finding allows us to understand the reasons why balanced bidirectional flow is efficient at low densities, but quickly leads to deadlock formation at high densities.

* feliciani@jamology.rcast.u-tokyo.ac.jp

I. INTRODUCTION

Given the rapid growth of the world's population, the urbanization process and the improvements in transportation, a growing number of people is moving with an increasing ease. As a consequence, large crowds routinely form during large events and congestion (both in terms of vehicles and people) is becoming an increasingly relevant problem in developing countries. Only in the last few years several accidents involving inefficient crowd management took the life of several hundreds of people, with Mecca (2015), Shanghai (2014) and Duisburg (2010) [1, 2] being some of deadliest accidents.

These facts, combined with an increasing interest on complex phenomena, have led many researchers to investigate the dynamics of large groups composed of self-driven particles such as crowds, herds, schools or swarms. A common characteristic in the dynamic of the different sorts of self-driven particles is that at some point collective behavior emerges, making it possible to describe the motion of the group's components as a whole [3, 4]. In biology such phenomena have been known for a long time and the concept of swarm intelligence is used to describe the emerging of collective behavior [5, 6].

Pedestrian dynamics (which considers humans) started as an experimental discipline in which data obtained from empirical observations were summarized in constructional guidelines [7]. However, during the last two decades the improvements in computer performances have led to the development of simulation techniques able to predict the general behavior of large crowds. While simple cases such as evacuation from a small door [8–10], bidirectional counter-flow [11–13] or cross-flow at intersections are still some of the most investigated cases (by means of both simulations and experiments), commercial software now allows to simulate pedestrians inside complex environments such as train stations or airports [14, 15].

In addition, thanks to the recent technological improvements, pedestrians' recognition and tracking is becoming feasible and surveillance cameras may be used on that purpose in the near future [16–20] (pedestrians avoidance technology is already available in some modern vehicles). However, besides the achievements of simulation models and the complexity of the systems simulated, the fundamental laws governing jam formation in pedestrian streams are still not completely understood. For this reason, the use of data gained from automatic pedestrian tracking and detection systems might be limited to very simple information such as average pedestrian speed or density. In this regard, recent studies have shown that average

quantities are not appropriate to describe crowd (or herd) behavior and employing statistical distributions may be more appropriate [21, 22]. Therefore, if jam (or in the extreme case stampede) prediction is sought by using basic pedestrian quantities (speed, density,...) it is important to understand the fundamental laws behind pedestrian collective phenomena.

In particular, for the case of bidirectional streams, influence of the different crowd parameters such as total flow, density and flow-ratio are not yet completely understood. In fact, some authors [23–25] found balanced bidirectional streams performing better than unidirectional ones, while different authors came to the opposite conclusion [11, 26–28]. Although it appears that the different conclusions are related to the different conditions under which the studies were performed, it is important to understand what are the conditions influencing the outcome of the experiment. Finally, to complete the short discussion on bidirectional streams, a recent study suggested that asymmetrically shaped walls can help organizing the pedestrians in lanes, although the study is based on computer simulation [29].

In our previous research [28, 30] we observed that flow-ratio has an important influence in determining the capacity of bidirectional flows (and that rotation is important for the dissolution of deadlocks). Besides this fact only little research has been dedicated in understanding how and why flow-ratio plays an important role in bidirectional streams. While a limited number of studies took flow-ratio into consideration to some extent [11, 23, 25, 27, 31], none of them provided numerical evidence to describe its influence on the total outcome of the pedestrian stream. In this paper we report the results of a supervised experiment involving pedestrians walking in opposite directions in a mock-corridor. The spontaneous lane formation process has been studied using the tracking data gained from video recording by employing statistical and fluid-dynamic methods. We hope that the methods introduced here can help researchers developing algorithms capable of predicting jam formation by using information obtained from cameras monitoring pedestrians in large venues or events.

II. EXPERIMENTAL SETUP

In order to understand qualitatively and quantitatively the influence of flow-ratio on bidirectional streams, we designed an experiment in which total flow and density are kept at fairly constant level among the different trials and flow-ratio is the only parameter being changed. The experiment was not designed to yield particular results or to confirm some

theories developed beforehand, but its only scope was to get as much data as possible (with high accuracy) therefore allowing a critical assessment of the information gained.

In this section the details concerning the geometrical layout and the execution of the experiment are presented and discussed.

A. Geometrical configuration and technical setup

A mock-corridor delimited with band partitions was created on a closed street in front of a tall building. The mock-corridor consisted of three main parts: the measurement area located in the center, two buffer zones located at each side of the central test section and two waiting areas located at both extremes of the buffer zones. A schematic description with dimensions for the whole floor setup are given in FIG. 1.

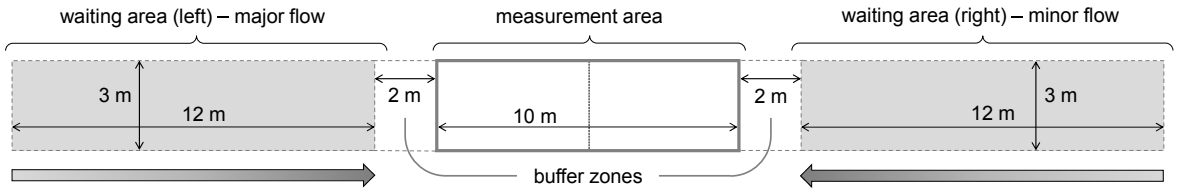

FIG. 1. Schematic representation and dimensions of the mock corridor used in the experiment.

The buffer zones were used to allow pedestrians reaching a stable speed before entering the measurement area. Although participants were actually already walking when inside the buffer zone, all the results presented in this study only refer to the data gained from the analysis of the measurement area (as the name suggests).

In each waiting area 9 columns were formed along its length by writing crosses on the ground (see FIG. 2 and FIG. 3). The distance between the different columns was of 1.5 m and the lateral distance between each cross was of 0.5 m (0.25 m between the external position and the section's border). The first column coincided with the boundary between the waiting area and the buffer zone. The crosses on the ground corresponded with the different starting positions used by the participants during the experiment. On each side a total of 54 positions were available, exactly matching the number of the participants.

Three cameras were placed in azimuthal position over the measurement area at an height of 21 m. A high-resolution wide-lens camera was used to record the movements of the pedestrians inside the measurement area (an example for an image taken from the central

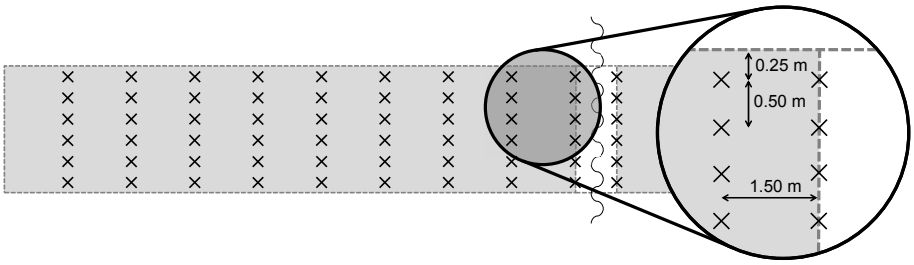

FIG. 2. Schematic representation of the grid employed in the waiting area.

FIG. 3. (Color online) Video frame taken before giving the start signal; participants are aligned in the waiting area. Measurement area, buffer zone and waiting area are clearly recognized by white lines. Because of the use of a wide-lens camera, images are distorted at the corners, but distortion in the measurement area is comparatively small. Participants on the left side wear yellow caps, participants on the right side red ones.

camera is given in FIG. 3; one may notice that the waiting areas are not covered from the camera's view). The remaining two cameras were pointing to each waiting area to allow keeping a record of the starting positions during each run (allowing an eventual later exclusion of runs in which participants were taking incorrect starting positions). All the cameras operated at 30 fps.

B. Participants

Participants were recruited among male university students on a voluntary basis and received a fixed compensation for the time spent during the experiment. The participants were given instructions concerning the procedures for the experiments, but they were not aware of the details and the type of measurements which will be gathered. The average age of the participants was of 21.03 years and their average free walking speed (measured at the

beginning of the experiment) was found being 1.40 ± 0.10 m/s (participants were asked to walk at natural speed, neither rushing nor walking at unnecessary low pace).

All the participants were wearing black T-shirts which were provided at the beginning of the experiment. In addition, depending on the waiting area they occupied, different cap colors were used: yellow for the members of the left waiting area (composing the major flow) and red for the pedestrians in the right waiting area (composing the minor flow).

During the whole experiment several breaks were performed to avoid exhaustion of the participants potentially leading to unwanted bias. Weather conditions were stable during the whole execution (partially clouded, about 25°C).

C. Execution and instructions

To start this section it is important to define all the physical quantities that will be used in the following descriptions. Density ρ refers to the number of people found in a given area and it is measured in persons/m^2. Flow q refers to the number of pedestrians passing through the full width of the corridor at a given location in a given time. It is measured in number of persons per meter width per second. In a bidirectional flow configuration, minor flow refers to the smallest flow found in both directions (sometimes called counter-flow), major flow is the largest flow. When considered apart, both minor and major flow are bidirectional and with opposite directions. The total flow is the sum of both minor and major flow and has a bidirectional nature (if both minor and major flow are present). Density and flow are traditionally linked from the fluid-dynamic identity:

$$q = \rho \cdot v \tag{1}$$

where v is the (average) velocity or the (average) walking speed in the case of pedestrians.

Finally, it is important to define the flow-ratio which will be employed in this study. Calling r the flow-ratio, it can be computed as:

$$r = \frac{\text{minor flow}}{\text{minor flow} + \text{major flow}} = \frac{\text{minor flow}}{\text{total flow}} \tag{2}$$

In order to vary the flow-ratio, 4 different configurations were tested: a purely unidirectional flow and 3 different configurations of bidirectional flow. Under the unidirectional flow configuration ($r = 0$ as minor flow is equal 0) participants in the waiting area took all the

available positions provided by the crosses on the ground. Once all participants were waiting in the correct positions a loud oral 'start' signal was given and all of them started to walk toward the exit located at the opposite side of the mock-corridor. Participants were asked to start simultaneously at the 'start' signal and the distance between them easily allowed such an instruction. After crossing the waiting area located at the opposite side, participants returned to their starting position by walking outside from the measurement area. Participants were asked to keep walking for a long distance after exiting the measurement area to avoid having jam formation at the end of the experiment. A schematic representation of the start positions for this unidirectional configuration is given in FIG. 4(a). 4 different runs were performed in the unidirectional layout and participants were asked to change their starting position on each run. Instructed personnel inspected the waiting area before the start of each run to avoid having the participants in repeating positions (e.g. keeping staying close to a friend/acquaintance or occupying always front/back positions).

In the first bidirectional configuration (see FIG. 4(b)) 9 participants were moved to the opposite waiting area. Under this configuration some empty places formed in the starting grid of the left waiting area (yellow/light gray). Participants waiting on the left side were asked to take whichever position they liked but to leave one empty spot for each column, while participants on the right side were asked to use one column per person. Supervising staff was present at both left and right waiting areas to avoid participants taking repeating position or starting in a queue configuration (especially in the minor flow). At the 'start' signal both groups started walking in opposite directions, thus forming a bidirectional flow inside the measurement area.

Safely assuming that members of the minor flow (right, symbol mn) and major flow (left, symbol mj) have similar free walking speed v, the flow-ratio for this configuration can be computed as:

$$r = \frac{\text{minor flow}}{\text{minor flow} + \text{major flow}} = \frac{v \cdot \rho_{mn}}{v \cdot (\rho_{mn} + \rho_{mj})} \tag{3}$$

$$= \frac{N_{mn}/A_{\text{wa}}}{(N_{mn} + N_{mj})/A_{\text{wa}}} = \frac{N_{mn}}{N_{tot}} = \frac{9}{54} = 0.167 \tag{4}$$

where N_{mn} and N_{mj} stand for the number of pedestrians in the minor and major flow respectively (N_{tot} is the total number of participants) and A_{wa} is the surface of the waiting

area (same in both directions). Data analysis of the results showed that actual values measured during the experiment are close and in line with the theoretical calculations presented above. This last bidirectional configuration, for which we will refer as 5/1 configuration (figures correspond to the number of persons per column on each side) was repeated 4 times.

Next, additional 9 people were moved from the left to the right side, as given in FIG. 4(c). This time, participants on the right side were asked to leave 2 spots empty for each column, while participants at the right side took 2 spots for each column. Again, this configuration, for which corresponding flow-ratio is $r = \frac{2}{6} = 0.333$, was repeated 4 times.

Finally, another 9 people were moved from left to right, thus creating the balanced bidirectional flow ($r = \frac{3}{6} = 0.5$) given in FIG. 4(d). This time both participants on the left and the right side had to take only half of the positions available, leaving 3 spots empty in each column. Balanced flow configuration was repeated 4 times also.

A summary of the different configurations with their codename and the corresponding flow-ratio is given in TABLE I. An illustrative example for a video frame taken before the start of the balanced flow experiment is given in FIG. 3.

TABLE I. Experimental configurations and their characteristics (UNI = unidirectional, BI = bidirectional).

Case	Type	Major flow (left)	Minor flow (right)	Flow-ratio
6/0	UNI	6 persons/column	0 persons/column	0.000
5/1	BI	5 persons/column	1 persons/column	0.167
4/2	BI	4 persons/column	2 persons/column	0.333
3/3	BI	3 persons/column	3 persons/column	0.500

D. Video post-processing

The frames obtained from the video recordings of the experiment were first crop and rotated to contain only the measurement area. Distortion of the lens was found being very limited in the measurement area, but to ensure the quality of the results corrections were taken during the tracking procedure. An example for a post-processed video frame taken

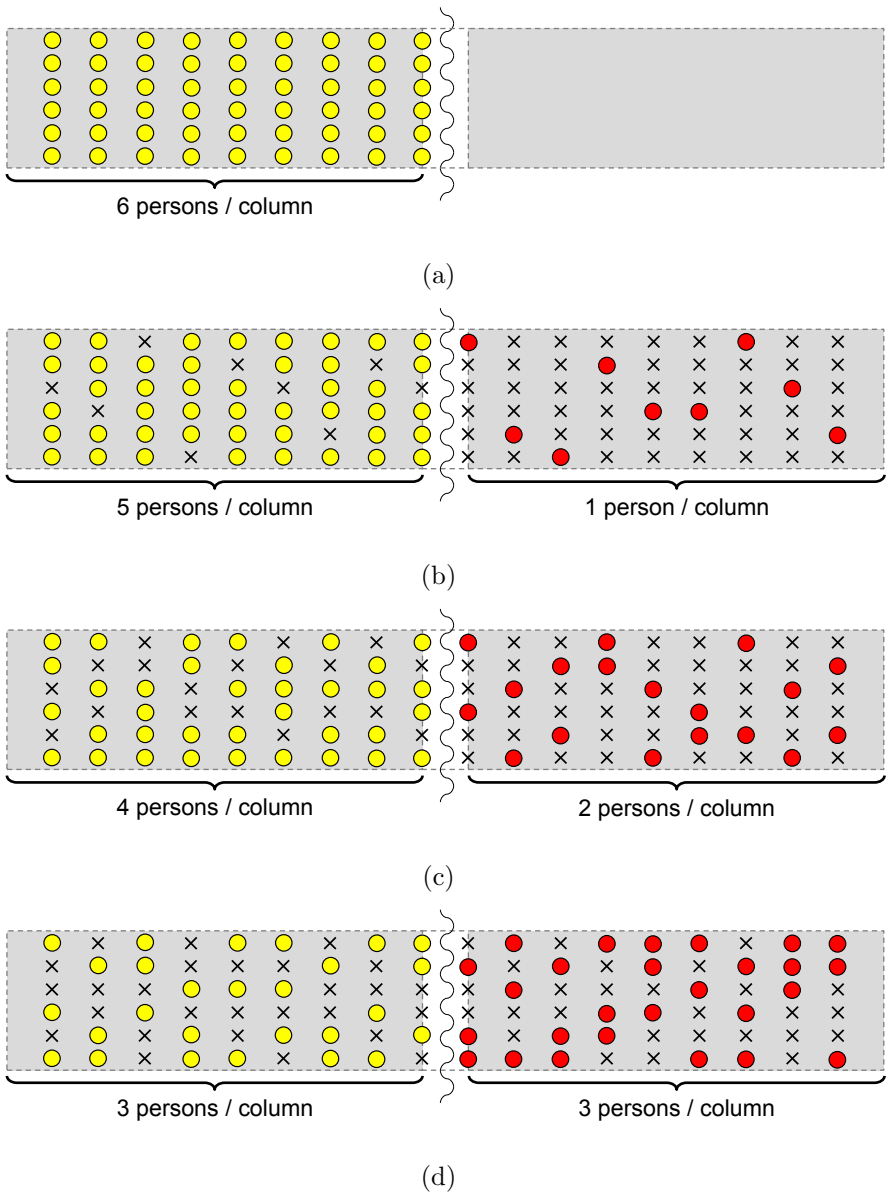

FIG. 4. (Color online) Starting positions during the different configurations: (a) unidirectional 6/0 configuration, (b) bidirectional 5/1 configuration, (c) bidirectional 4/2 configuration and (d) bidirectional 3/3 configuration. Positions given in the diagram does not necessarily coincide with the actual positions taken by participants during the experiment and are only for illustrative purpose. Crosses represent empty positions, while circles stand for occupied positions. Yellow (light gray) circles symbolize participants of the major flow and red (dark gray) circles are representative of the minor flow.

during the balanced bidirectional flow experiment is given in FIG. 5.

FIG. 5. (Color online) Example of a video frame taken during the balanced bidirectional flow experiment. Measurement area is marked with white lines, right walkers (originating from the left waiting area) have yellow (light gray) caps and left walkers (starting in the right waiting area) red (dark gray) caps.

After obtaining the relevant frames centered on the measurement area, images were analyzed using the PeTrack [32] software, which allows to obtain the position of each participant for all the time frames considered. Velocities were computed using the position data for each pedestrian, but, in order to remove short-term fluctuations and tracking imperfections a time period of 3 frames was considered to calculate the average velocity. This means that, given the original video frame rate of 30 fps, a time period of 0.1 s is considered for velocity calculation, sufficiently small to consider rapid changes in trajectory or pace. Densities were computed using the Voronoi cells method [33] to increase the accuracy of the results.

A complete analysis of the data obtained showed that, as planned and theoretically predicted, maximum total flow reached at the center of the measurement section was comparable for all the cases considered (around 1.6-1.7 $(m \cdot s)^{-1}$), while maximum density reached has been of about 1.5 person m^{-2}. Total flow and density time profiles computed at the center of the measurement area also showed similar patterns in all configurations and runs.

Videos of the experiment are provided as supplemental material of this paper [34]. In the videos, the naming used in TABLE I is used to distinguish between each configuration and roman letters (ABCD) are used to distinguish between each repetition (A being the first run, B the second and so on).

III. RESULTS

In this section the main findings of the experiment are presented and discussed in detail. The first part includes a general discussion about the qualitative characteristics of the flow observed and an initial analysis using the quantities typically used to analyze pedestrian streams. Later, particular properties and additional quantities are used to describe the main features of the bidirectional flow analyzed.

A. Pedestrians trajectories and crossing time

First of all, in order to compare the different cases we wish to get a general idea of the way pedestrians behave inside the mock-corridor. FIG. 6 shows the trajectories of the pedestrians observed in the different configurations from the beginning to the end of a selected run, i.e. considering the full length of the experiment. The color in each trajectory indicates the horizontal speed (x-velocity) for the given moment/position. Here, it has to be reminded that for each configuration 4 different runs were performed, so the trajectories given below are only for the most representative example of each configuration and slight differences exist for each run.

Although FIG. 6 overlaps different time frames and therefore it is not sufficient for a complete analysis, some aspects which will be discussed later can already be observed here. In particular, in the unidirectional 6/0 case it can be observed that people tend to keep their original position and simply keep going straight. In fact, especially in the left side of FIG. 6(a), 6 different lanes are easily recognized, which eventually become slightly mixed at the exit on the right side. In FIG. 6(b) (bidirectional 5/1 configuration) a more complex flow pattern is observed as pedestrians of the minor flow (having negative red/dark gray velocity) have to take some deviations to overcome the incoming large counter-flow. Although some stable lanes can be observed (by noticing that at the left side trajectories of the minor flow tend to occupy an area unused by the major flow), in general the flow behavior can be described as unorganized since trajectories of the major and minor flow overlaps in different locations.

The bidirectional 4/2 case (FIG. 6(c)) shows a more ordered scenario. Members of the minor flow now tend to organize themselves in groups by forming a more limited number of

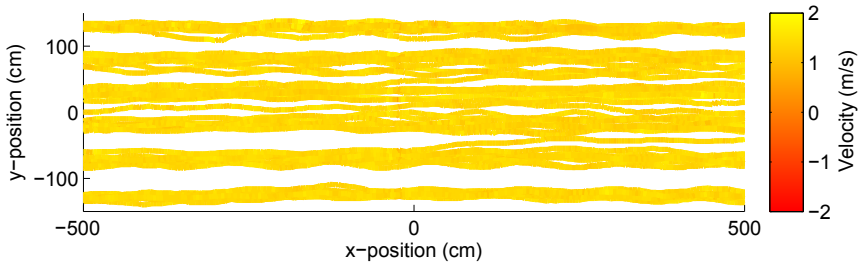

(a)

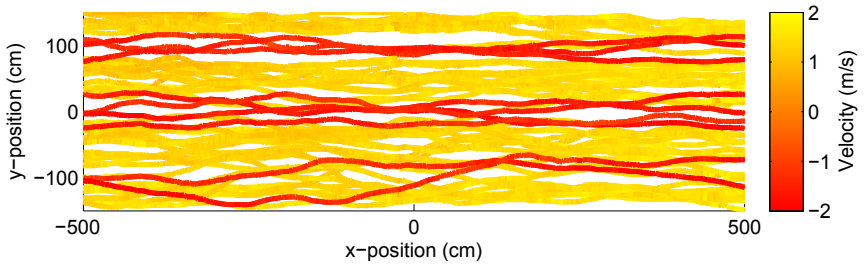

(b)

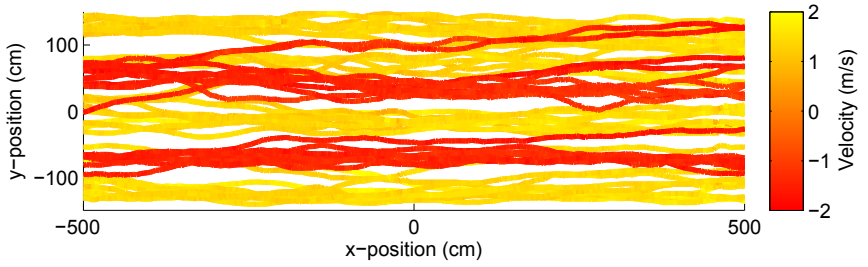

(c)

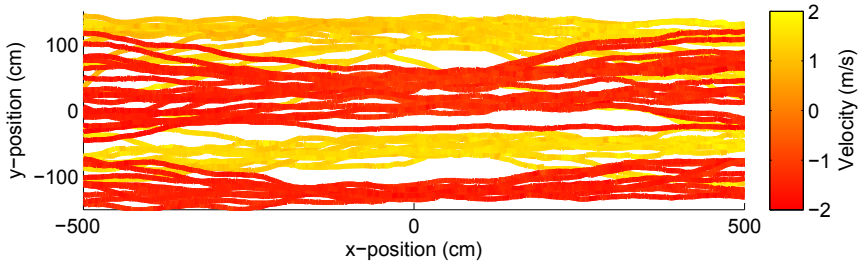

(d)

FIG. 6. (Color online) Trajectories recorded in a selected run for each of the different configurations: (a) 6/0 configuration, (b) 5/1 configuration, (c) 4/2 configuration and (d) 3/3 configuration. Path color (gradation) indicates the x-component of the velocity. It is important to remind that each configuration was repeated 4 times, so the trajectories represented here are only for reference. Major flow (positive velocity, yellow/light gray) goes from left to right, minor flow (negative, red/dark gray) from right to left.

lanes and taking a defined portion of the corridor. Although in the right side of FIG. 6(c) pedestrians of the minor flow show some individual behavior, more organized lanes are formed at the exit (left side). The emergent lane formation mechanism is particularly recognizable in FIG. 6(d) (balanced bidirectional flow), where each group (left and right walkers) show a similar behavior by forming 2 lanes in each direction which does not change during the full length of the experiment (trajectories barely overlap in the central part of the measurement area).

We can now consider the crossing time, i.e. the time required to go from one side to the other of the measurement section, given in TABLE II. For each configuration the crossing time measured for each pedestrian in the 4 runs was recorded and the corresponding average and 1σ deviation are reported. Separate figures are given for the major, the minor flow and the whole group of pedestrians.

TABLE II. Average crossing time for the different configurations (UNI = unidirectional, BI = bidirectional) and the different groups. Uncertainties are 1σ standard deviation.

Case	Type	Flow-ratio	Crossing time		
			Complete group	Major flow	Minor flow
6/0	UNI	0.000	7.273 ± 0.319 s	7.273 ± 0.319 s	–
5/1	BI	0.167	7.309 ± 0.561 s	7.398 ± 0.465 s	6.870 ± 0.768 s
4/2	BI	0.333	7.266 ± 0.580 s	7.365 ± 0.573 s	7.070 ± 0.549 s
3/3	BI	0.500	7.326 ± 0.592 s	7.488 ± 0.613 s	7.164 ± 0.525 s

The average crossing time taken from the complete group of pedestrians does not show any significant trend, thus suggesting that average values are inappropriate to describe overall characteristics of pedestrians streams. On the other side the dispersion shows a small but clear trend in connection with the flow-ratio, with the unidirectional flow case having the most uniform crossing time and the balanced case having the largest dispersion.

When major and minor flows are considered separately it is interesting to notice the opposite trend observed in the variance. While variance of the major flow increases with the flow-ratio (similarly to the trend of the complete group), variance of the minor flow has the lowest value in the balanced bidirectional configuration and shows the largest dispersion in the 5/1 configuration. In the case of the minor flow a linear trend is observed in the average

value too, while for the major flow it is difficult to recognize a particular pattern, although it appears that, in general, bidirectional cases have higher crossing times compared to the unidirectional case.

B. Fundamental diagram

Before starting the statistical analysis we wish to give a look to the fundamental diagram to make sure that the different configurations are equivalent in terms of the flow regime observed and to understand the role of the minor and the major flow. Fundamental diagram has been used for decades in vehicular traffic and its application to pedestrian traffic has been also considered [35]. However, although single lane unidirectional flow can be easily studied using the fundamental diagram, its application to more complex systems is debated. Nonetheless, for fairly simple configurations as the one considered here, its use may be appropriate.

FIG. 7 shows the fundamental diagrams of the different configurations plotted in the same graph. Diagrams were generated by taking the average density and x-velocity (making up the flow by multiplication) measured during each time frame (i.e. every 0.33 s) from the beginning to the end of each run. Each dot in FIG. 7 is therefore obtained by considering the average density and x-velocity in a given time frame. To compute the density for each pedestrian Voronoi cells were used (see also [36]). Only fully defined cells were used in the analysis (Voronoi cells for pedestrians entering and leaving the measurement area are excluded in the analysis). In this case all the 4 runs of each configuration have been used to create a single fundamental diagram.

A first glance clearly reveals that uncongested flow was observed during the experiment. All the graphs show, on average, an almost-linear behavior with most of the dots being aligned along a fictional line starting from the origin. By analyzing FIG. 7 only, one may conclude that all configurations are equivalent, with only a slightly larger dispersion found for the balanced bidirectional flow. These qualitative remarks are supported by numerical evidence obtained by performing a linear regression on the fundamental diagrams and measuring the dispersion resulting from the average slope. Results given in TABLE III shows that especially for the bidirectional cases there is no significant difference between the fundamental diagrams.

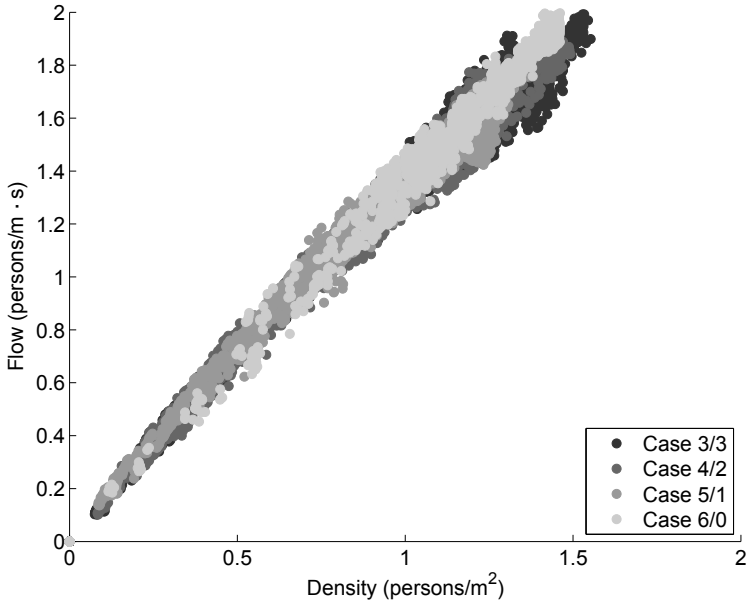

FIG. 7. Comparison of the different fundamental diagrams; no differentiation is made between minor and major flow. Uncongested, comparable flow was observed in all the cases. Without further investigations differences between the different configurations cannot be easily identified.

In this regard, Zhang et al. [11], conducting a similar experiment with a larger number of participants, came to the same conclusion, i.e. that no difference can be found between bidirectional fundamental diagrams. Zhang et al. found clear differences between uni- and bidirectional fundamental diagrams, which can be recognized only in a very little extent in this study (possibly because of the relatively uncongested nature of the experiment reported here).

To grasp any difference between the different configurations we can now compare the fundamental diagrams by considering separately minor and major flow. For each time frame, average density and x-velocity were computed separately for each class of pedestrians and results were plotted using different colors (gradations) as shown in FIG. 8. In this case, for each time frame, two dots are generated: one using the density and x-velocity of the major flow and the other one using data of the minor flow. Again, the 4 runs were combined to obtain a single fundamental diagram for each configuration.

Probably the most relevant feature to be recognized in the fundamental diagrams is the high dispersion of red (dark gray) dots (minor flow) observed in the 5/1 configuration at high densities (see FIG. 8(b)). This explains the results observed for the crossing time and

TABLE III. Slope resulting from the linear regression of fundamental diagrams given in FIG. 7 (complete group) and FIG. 8 (major and minor flow). Dispersion is measured using the root mean squared error.

Case	Velocity		
	Complete group	Major flow	Minor flow
6/0	1.341 ± 0.047 m/s	1.341 ± 0.047 m/s	–
5/1	1.286 ± 0.057 m/s	1.284 ± 0.059 m/s	1.313 ± 0.160 m/s
4/2	1.300 ± 0.059 m/s	1.286 ± 0.067 m/s	1.344 ± 0.077 m/s
3/3	1.267 ± 0.070 m/s	1.237 ± 0.072 m/s	1.300 ± 0.087 m/s

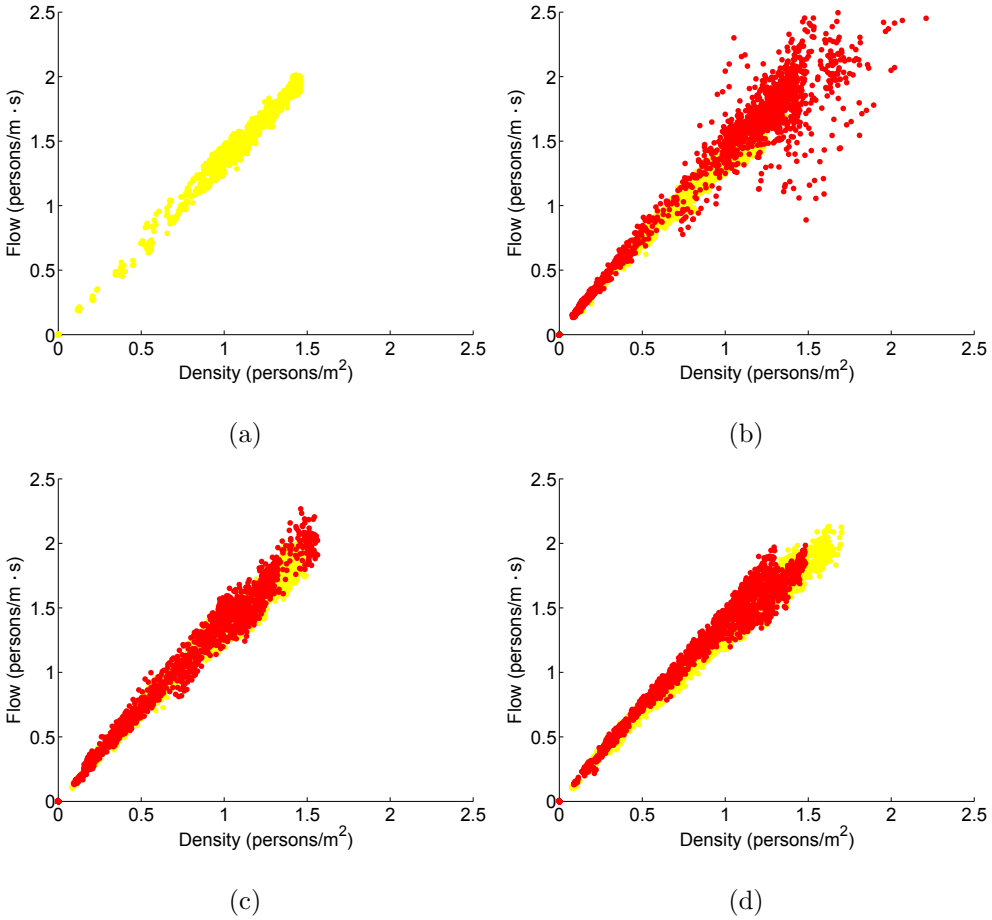

FIG. 8. (Color online) Fundamental diagrams for each configuration: (a) 6/0 configuration, (b) 5/1 configuration, (c) 4/2 configuration and (d) 3/3 configuration. Diagrams were obtained by combining the results of the 4 runs in each case. Dots' color indicates the group considered: yellow (light gray) stands for major flow and red (dark gray) for minor flow.

indicates that members of the minor flow have to continuously slow down/speed up to find their way through the incoming larger major flow. In contrast, the unidirectional case, shows a very compact shape, with most of the dots to be found in a limited surface. Interestingly, except for the larger dispersion observed in the 5/1 configuration, minor and major flows show very similar characteristics when compared using the fundamental diagram, suggesting that further investigations are required. These remarks are reflected by the numerical data given in TABLE III.

C. Bidirectional flow mechanisms

Because the fundamental diagram does not give information concerning the mechanisms observed in bidirectional flows, we need to consider different quantities. But before continuing, it is important to define the several steps leading to the formation of lanes in bidirectional streams.

In fact, our experiment starts as a combination of unidirectional streams with opposite directions and only later a bidirectional flow is formed. Six different time instants are relevant for the experiment considered (for some of them a representative image is given in FIG. 9):

- $t_0 = 0$: the first pedestrian (either minor or major flow) enter the measurement area (time measurement starts from here)
- t_1: the leading pedestrians of the major and minor flow cross each other's (see FIG. 9(a))
- t_2: pedestrians start exiting from both sides (see FIG. 9(b))
- t_3: the last pedestrian either of the major or the minor flow enters the measurement area (see FIG. 9(c))
- t_4: the last pedestrians of each group leave behind each other's (see FIG. 9(d))
- t_5: the last pedestrian leave the measurement area (time is stopped, from now on no data are taken).

The processes observed for each interval between the time instants considered above can be described as follows:

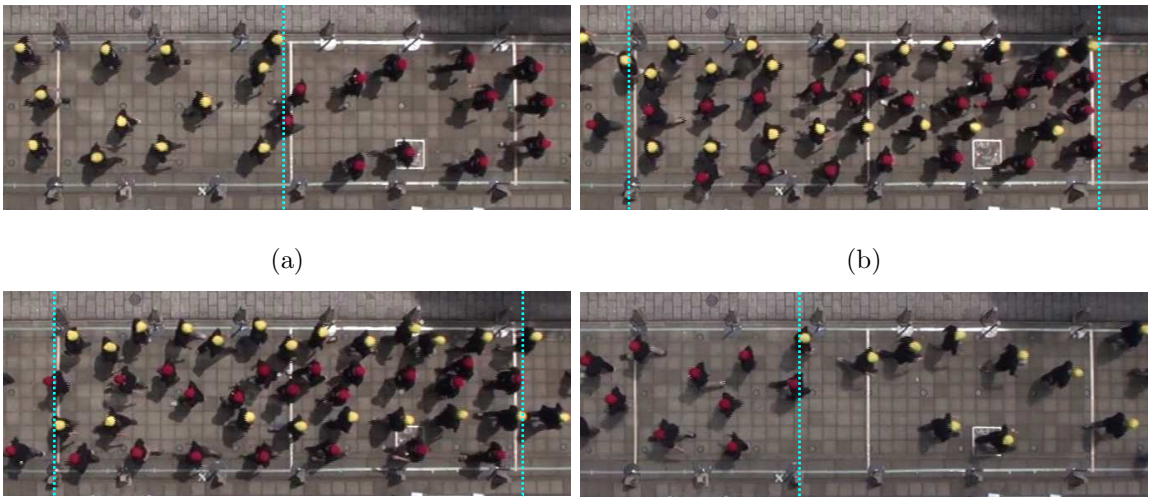

(a) (b)

(c) (d)

FIG. 9. (Color online) Relevant moments during the process of lane formation and dissolution in a balanced bidirectional flow: (a) time t_1 (beginning of lane formation), (b) time t_2 (beginning of full bidirectional flow), (c) time t_3 (beginning of lane dissolution) and (d) time t_4 (end of bidirectional flow). Major flow pedestrians wear yellow (light gray) caps, minor flow participants use red (dark gray) caps.

- Phase 1 (t_0 - t_1): unidirectional free-flow. Major and minor flow can be considered as two separate unidirectional streams, pedestrians have not yet started physically interacting with each other.

- Phase 2 (t_1 - t_2): lane formation. Pedestrians moving in different directions interact with each others and lanes are formed.

- Phase 3 (t_2 - t_3): full bidirectional flow. The whole measurement section is filled with pedestrians of the major and minor flow, a bidirectional stream can be observed in all the x-positions of the section considered.

- Phase 4 (t_3 - t_4): lane dissolution. Lanes are being dissolved and in parts of the measurement section unidirectional flow is observed.

- Phase 5 (t_4 - t_5): unidirectional free-flow. Again, minor and major flows can be regarded as two separate unidirectional streams.

Because each phase is conceptually different, from now on we wish to consider each

time interval separately and investigate if there are characteristic features describing the phenomena observed in each of them.

To allow a comparison with the quantities observed for unidirectional flow (6/0 configuration), we decided to divide the time interval in a similar way, although the phenomena observed are the same in all the phases. At the scope, instead of considering the incoming counter flow, the center-line ($x = 0$) is used to determine the beginning of a phase and the start of the following one in the case of unidirectional flow.

D. Velocity distribution

x-velocity

First of all it is important to examine the x-velocity, thus the velocity of the forward motion. For all the cases considered a Gauss distribution was observed and confirmed by fitting with the Gaussian function. This is not surprising and it has been often reported in the literature [7, 37–39]. It is therefore appropriate to measure velocities in terms of average value and 1σ variance. The results for the x-velocity during the different phases and in function of the flow-ratio are reported in FIG. 10; colors refers to the minor and major flow as used for the previous graphs. To make comparison easier, absolute values are used for the average x-velocity.

During the first phase, the minor flow shows a larger average velocity compared to the one of the major flow. The difference is particularly large for low flow-ratios. This result should not come as a surprise because, during phase 1, both minor and major flows can be regarded as separated unidirectional flows whose velocities are related with the densities observed. As a consequence, the low density of the minor flow comes with a higher velocity. Variances during phase 1 are comparable and relatively low, showing that pedestrians are moving in a uniform way.

During phase 2 (lane formation) the average x-velocities clearly drop, while there is an increase in the variance observed, especially in the case of the minor flow. Although in general the minor flow still has a higher x-velocity compared to the major flow, a wide range of velocities is observed.

In phase 3 (full bidirectional flow) there is an additional increase in the variance measured,

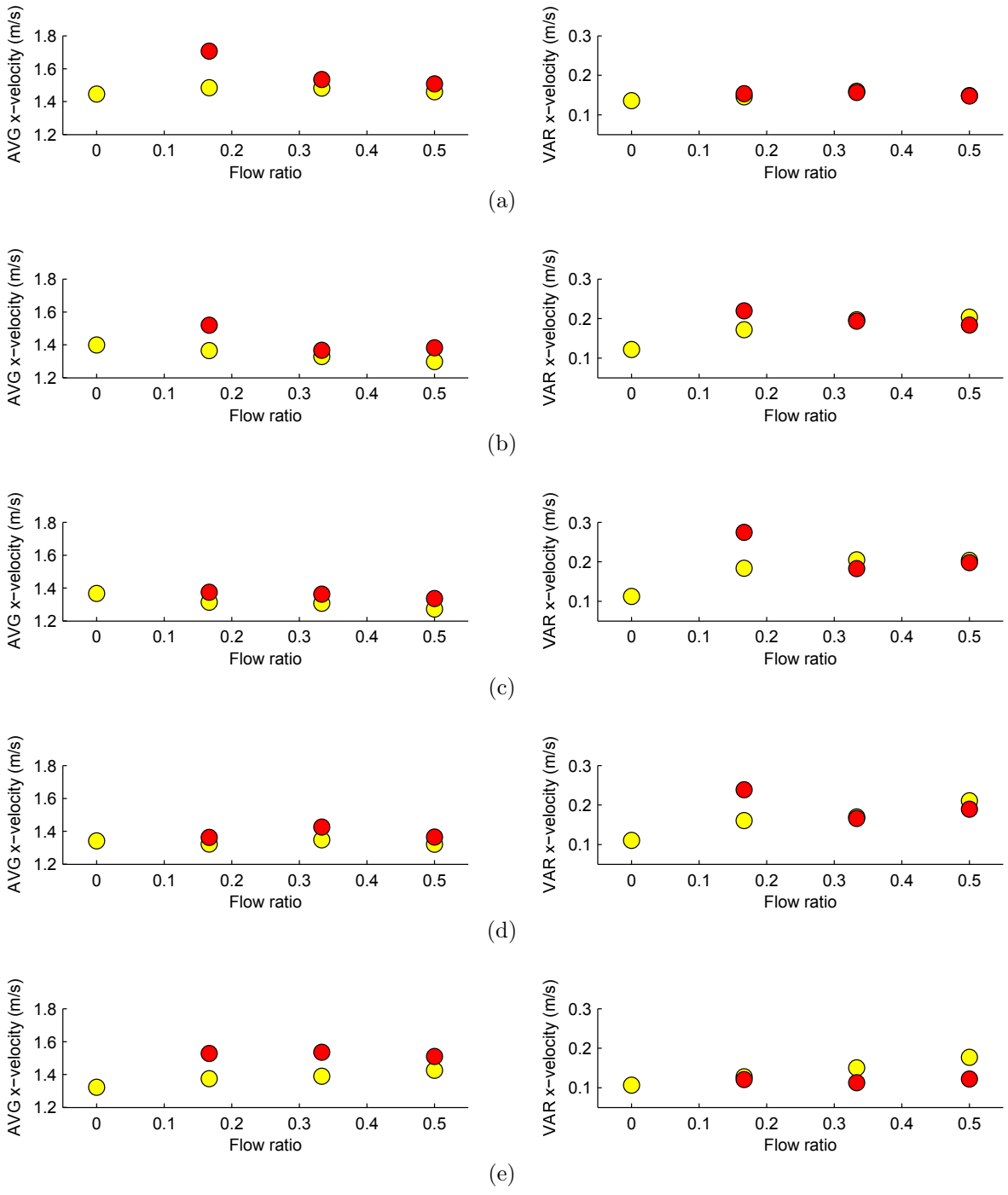

FIG. 10. (Color online) x-velocity for the different phases: (a) unidirectional free-flow, (b) lane formation, (c) full bidirectional flow, (d) lane dissolution and (e) unidirectional free-flow. Yellow (light gray) dots refer to the major flow and red (dark gray) dots to the minor flow. AVG stands for average, VAR for variance.

while the average values stay almost constant. Interestingly, the variance of the major flow increases with an increase in flow-ratio, with the variance of the minor and major flow being almost identical for balanced bidirectional flow. The difference in variance is particularly clear for the 5/1 configuration (flow-ratio = 0.167).

In phase 4 (lane dissolution) the average x-velocity slightly increases and the variance decreases, showing an opposite behavior to the process which led to lane formation.

Finally, in phase 5, as the flow becomes unidirectional, the velocities grow again, while the variance drops, showing again a fairly uniform motion.

y-velocity

Although pedestrians' velocity clearly has a larger x-component, it is important to consider the y-component also, because it accounts for the lateral motion measured during each phase. In presenting the results for the y-velocities (given in FIG. 11), we used the absolute value to compute the average, while the variance was computed using the nominal value. The absolute value is required to account with the same weight left and right movement, which would result in an average y-velocity close to 0 otherwise.

Phases 1 and 2 show similar profiles concerning both the average and the variance of the y-velocity. In each case, both the average and the variance of the major flow grow with an increase in flow-ratio, showing that for the balanced case the major flow requires more lateral adjustments compared to the homogenous unidirectional flow or low flow-ratio.

It is interesting to notice how the trend changes when a full bidirectional flow is formed in phase 3. With a partial exception of phase 4, the full bidirectional flow is the only moment in which the y-velocity (both average and variance) decreases with flow-ratio. This indicates that the balanced flow is clearly more stable than the cases with low flow-ratio and the level of y-velocity reached by the balanced flow is comparable to the one of the unidirectional flow, thus confirming the hypothesis stated by some researchers that once lane are formed, bidirectional flow can be regarded as two unidirectional flows moving in opposite directions and taking different portions of space.

Later, from phase 4 to 5, the behavior observed during lane formation is repeated in the opposite way, restoring the growing y-velocity profile observed for the variance of the major flow in phase 1.

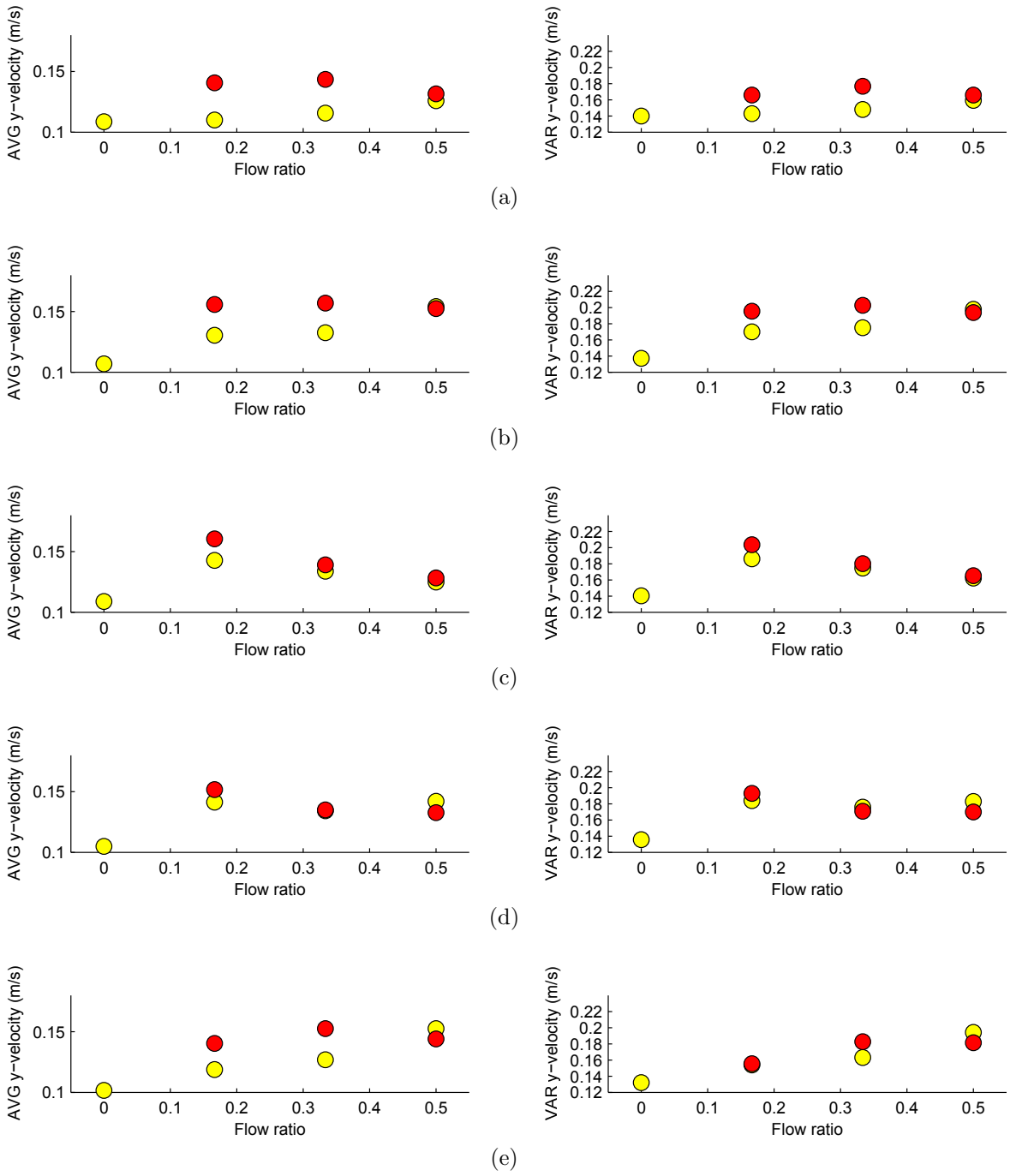

FIG. 11. (Color online) y-velocity for the different phases: (a) unidirectional free-flow, (b) lane formation, (c) full bidirectional flow, (d) lane dissolution and (e) unidirectional free-flow. Yellow (light gray) dots refer to the major flow and red (dark gray) dots to the minor flow. AVG stands for average, VAR for variance.

ANOVA test on velocity

A two-factors analysis of variance (two-way ANOVA) was conducted to test the combined potential effect of flow-ratio and phase on the x- and y-velocity of both the minor and major flows. Statistics have been conducted at the $p < 0.05$ level considering the 4 repeated runs. Results are presented in TABLE IV, where combinations with a statistically significant outcome are given in bold text.

TABLE IV. Two-way ANOVA test on the combined potential effect of flow-ratio and phase on the different aspects of velocity. Components having a statistically significant effect ($p < 0.05$) are given in bold (AVG = average, VAR = variance).

Flow-ratio		Major flow	Minor flow
AVG	x-velocity	$F(3, 60) = 0.686$, $p = 0.564$	$\boldsymbol{F(2, 45) = 5.912, p = 0.005}$
	y-velocity	$F(3, 60) = 0.469$, $p = 0.705$	$F(2, 45) = 0.214$, $p = 0.808$
VAR	x-velocity	$\boldsymbol{F(3, 60) = 29.80, p < 0.001}$	$\boldsymbol{F(2, 45) = 7.005, p = 0.002}$
	y-velocity	$\boldsymbol{F(3, 60) = 28.39, p < 0.001}$	$F(2, 45) = 1.144$, $p = 0.328$
Phase		**Major flow**	**Minor flow**
AVG	x-velocity	$\boldsymbol{F(4, 60) = 25.62, p < 0.001}$	$\boldsymbol{F(4, 45) = 20.55, p < 0.001}$
	y-velocity	$F(4, 60) = 0.793$, $p = 0.534$	$F(4, 45) = 2.525$, $p = 0.054$
VAR	x-velocity	$\boldsymbol{F(4, 60) = 6.068, p < 0.001}$	$\boldsymbol{F(4, 45) = 15.59, p < 0.001}$
	y-velocity	$\boldsymbol{F(4, 60) = 6.002, p < 0.001}$	$\boldsymbol{F(4, 45) = 4.465, p = 0.004}$
Interaction		**Major flow**	**Minor flow**
AVG	x-velocity	$\boldsymbol{F(12, 60) = 2.385, p = 0.014}$	$\boldsymbol{F(8, 45) = 2.358, p = 0.033}$
	y-velocity	$F(12, 60) = 1.059$, $p = 0.410$	$\boldsymbol{F(8, 45) = 2.474, p = 0.026}$
VAR	x-velocity	$F(12, 60) = 1.754$, $p = 0.078$	$F(8, 45) = 1.543$, $p = 0.170$
	y-velocity	$\boldsymbol{F(12, 60) = 2.792, p = 0.004}$	$\boldsymbol{F(8, 45) = 2.362, p = 0.032}$

In general both flow-ratio and phase have a statistically significant effect on the variance of both x- and y-velocity, with the relationship being particularly relevant for the phase factor. Average velocity seems to be less affected by both flow-ratio and phase. Generally speaking, although qualitative analysis based on the previous graphs suggested that y-velocity follow a particular pattern, statistical analysis indicate that flow-ratio and phase have a more

significant effect on x-velocity. Finally a significant interaction among both factors was found on the average x-velocity and the variance of the y-velocity, partially in line with the qualitative remarks from the previous sections. In general, minor and major flow seem to be equally affected by flow-ratio and phase.

E. Time lapse

We wish to continue the statistical treatment by using a different quantity. Some researchers [21, 22] showed that pedestrians (or animals) interactions are governed by power laws and in particular time lapse distribution (i.e. the time interval resulting from the passage of two consecutive pedestrians through a given position, obtained by measuring the time between consecutive pedestrians passing the same x-location) can be described using a power function.

We want therefore to check this hypothesis by using our dataset. FIG. 12 show the cumulative density function (CDF) obtained for different positions and for the different configurations considered in this experiment. In each case, minor and major flow are considered separately and entrance and exit are relative to the initial position of both groups.

For each case the time lapse distribution fits well with the exponential function given by:

$$CDF(\Delta t) = \alpha \mathrm{e}^{\beta \Delta t} \tag{5}$$

where Δt represents the time lapse and α and β are parameters to be determined empirically. The wider distribution of the minor flow results from the lower density of the initial group and both distributions become very similar in the case of perfectly balanced flow. The time lapse CDF – flow-ratio relationship is summarized in FIG. 13, where the β parameter giving the width of the distribution is plotted against the flow-ratio for both minor and major flows.

As FIG. 13 clearly shows, in all positions, the width of time lapse distribution of the minor flow decreases with an increase of flow-ratio which is ultimately connected with the density of each group considered separately. The opposite behavior is observed in the major flow, which has its density decreasing with an increase in flow-ratio, ultimately leading to a less compact and heterogeneously distributed group. Both major and minor flow lines intersect close to the balanced bidirectional flow, where both densities are equal. Concluding, we

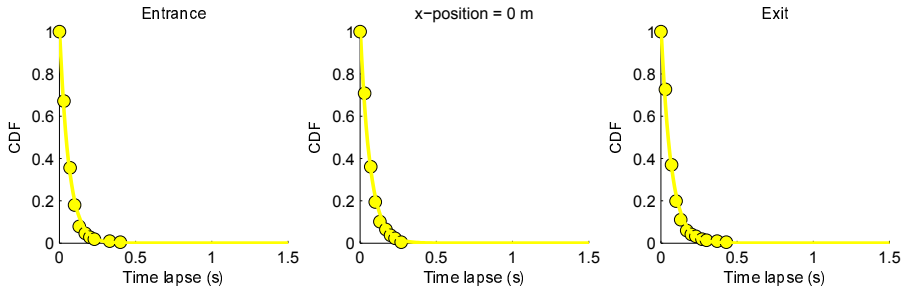

(a)

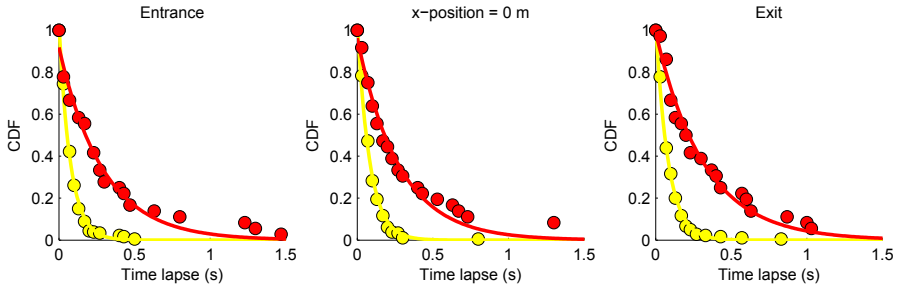

(b)

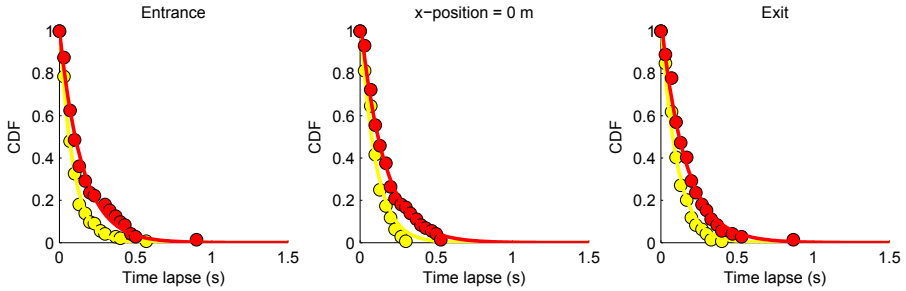

(c)

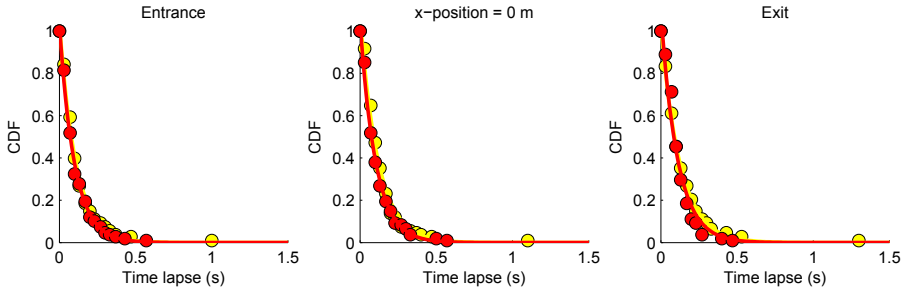

(d)

FIG. 12. (Color online) Time lapse distribution for the different configurations: (a) 6/0 configuration, (b) 5/1 configuration, (c) 4/2 configuration and (d) 3/3 configuration. Each distribution fits well with the exponential function. Yellow (light gray) is used for the major flow and red (dark gray) for the minor flow. CFD stands for cumulative density function.

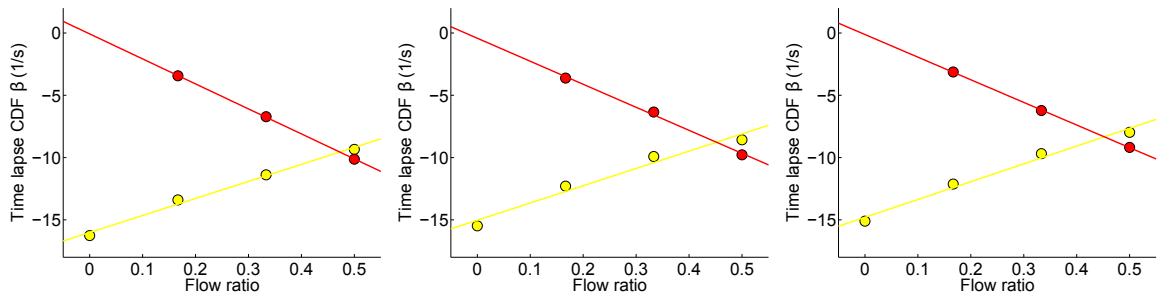

(a) (b) (c)

FIG. 13. (Color online) Time lapse distribution width in function of the flow-ratio for different positions: (a) entrance, (b) x-position = 0 m and (c) exit. Yellow (light gray) is used for the major flow and red (dark gray) for the minor flow.

could confirm that time lapse distribution can be described using power laws, but it is difficult to grasp the nature of the phenomena observed only based on this distribution. In the next sections we will discuss different quantities which may contribute in gaining a wider understanding of bidirectional flow.

F. Order parameter

Until now only statistical or one-dimensional quantities have been considered; but we want now to extend the discussion on two-dimensional quantities, which may become useful to describe more complex phenomena. First of all, we will introduce the order parameter, a quantity proposed by Rex et al. [40] to describe lane formation in colloidal fluids. The same order parameter has been used by Nowak et al. [41] to detect lane formation in simulated bidirectional pedestrian flows, thus showing the applicability to pedestrian dynamics.

To simplify the calculation of the order parameter it is convenient to have a computational grid comprising the average velocity recorded in each location (cell) over a finite time period. We can therefore use the data gained in the experiment and discretize the measurement area in cells having a fixed side length. In this study a cell size of 0.2 m was chosen, taking the balance between having a small accurate mesh and filling enough cells to allow a meaningful calculation of the different parameters (in addition, the size chosen is half the typical cell width used in pedestrian simulations). In each cell location, the average velocity is computed for the 5 phases considered so far. As an illustrative example, the velocity grid obtained

for a single run of the balanced bidirectional flow is given in given in FIG. 14 (the case considered here corresponds to the trajectories given in FIG. 6(d)).

The bar graph on the right side of FIG. 14 gives the overall velocity profile taken along the whole x-length for the different y-positions (or rows). As shown in FIG. 14(c), the bar graph helps counting the number of lanes and the direction for each.

By taking FIG. 15 as reference and using the velocity values shown in FIG. 14, the (global) order parameter can be readily computed applying the following equations. First, the local order parameter ϕ_j is computed for each row according to the below equation:

$$\phi_j = \left(\frac{n_j^L - n_j^R}{n_j^L + n_j^R} \right)^2 \tag{6}$$

where n_j^L and n_j^R represent the number of left and right walkers in the jth row. Finally, the global order parameter Φ can be computed as:

$$\Phi = \frac{1}{N} \sum_{j=1}^{N} \phi_j \tag{7}$$

where N represents the number of rows. Order parameter is always positive, even in the extreme case of random movement and becomes 0 only for vertically aligned patterns. For unidirectional or perfectly aligned bidirectional flows (where each row is occupied by only one class of pedestrians) the order parameter equals to 1. Any value in the middle can be used to measure the stratification of a bidirectional flow.

Order parameter can therefore be used to measure the alignment of lanes formed in the different configurations. Given its definition, it is however meaningful to only consider the full bidirectional phase, since non fully-developed cases would lead to values depending on the number of pedestrians in each group and not representing the nature of the phenomenon being observed. Results for the order parameter computed in the different configurations during phase 3 is given in TABLE V.

In TABLE V a linear relationship between flow-ratio and order parameter is shown, with the order parameter increasing as the flow becomes balanced. However, uncertainties have fairly large values, therefore making it difficult to make clear distinctions. A one-way AREVA analysis on the order parameter confirms that the influence of flow-ratio is not significant ($F(2,9) = 0.862$, $p = 0.455$).

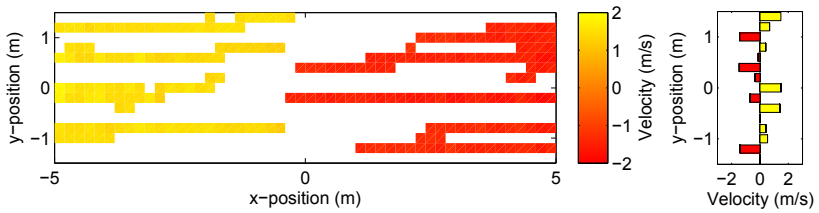

(a)

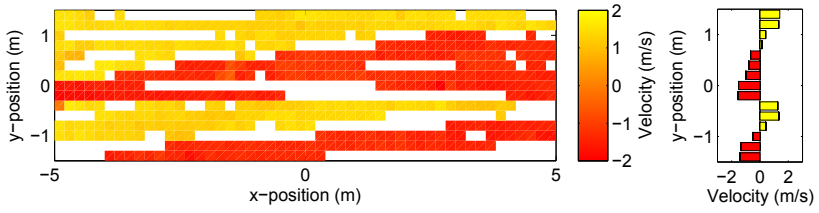

(b)

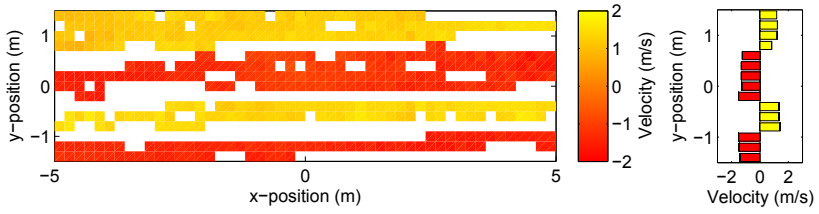

(c)

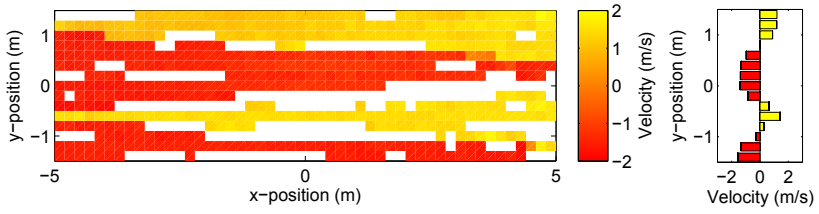

(d)

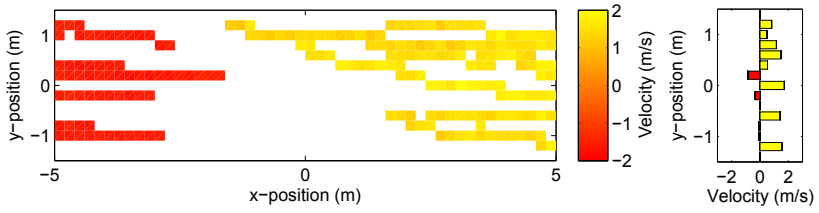

(e)

FIG. 14. (Color online) 2D plot of the average x-velocity in different locations for each phase: (a) unidirectional free-flow, (b) lane formation, (c) full bidirectional flow, (d) lane dissolution and (e) unidirectional free-flow. The bar graph on the right side gives the average velocity across the different rows. Grid size is 0.2 m $\times$ 0.2 m and white spots indicate unavailable data. Major flow has a yellow (light gray) gradation and minor flow is represented with red (dark gray) gradation.

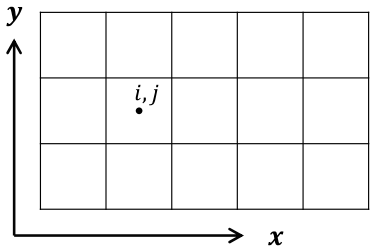

FIG. 15. Computational grid used for the computation of the order parameter.

TABLE V. Order parameter for the different configurations during full bidirectional flow. 6/0 configuration is omitted because order parameter is 1 by definition. Uncertainties are 1σ standard deviation.

Configuration	Flow-ratio	Order parameter
5/1	0.167	0.824 ± 0.130
4/2	0.333	0.881 ± 0.131
3/3	0.500	0.938 ± 0.105

Still, a qualitative visual analysis of the video recordings suggests that indeed more ordered lanes are observed in the balanced case, where the order parameter is very close to unity. The results suggest that the order parameter might be used to grasp a more general image on bidirectional pedestrian flow, but its accuracy is limited and in absence of large changes (very disorganized scenarios were not considered here) differences can be statistically insignificant. In addition, its use is confined only to horizontal bidirectional flows or simple cases making a practical application limited.

G. Vector field and rotation

To overcome some of the limitations of the order parameter and allowing a combined analysis of both x- and y-velocities, an additional method is proposed.

The concept of rotation (or vorticity, turbulence) is not new in pedestrian dynamics and several authors have used different mathematical methods to analyze crowd using this principle [2, 42, 43]. In this regard, it can be useful to consider the same grid used for the order parameter, but create a vector field by using x- and y-velocities in each cell. From the resulting vector field $\vec{F}(x, y)$ the rotation $\vec{R}(x, y)$ can be computed in each position using

the following equation:

$$\vec{R}(x,y) = \begin{pmatrix} r_x \\ r_y \\ r_z \end{pmatrix} = \vec{\nabla} \times \vec{F}(x,y) \tag{8}$$

Since only x- and y-values are used, r_x and r_y will be 0 and only r_z can deliver useful information. In addition, since right-hand and left-hand rotations in the vector field result in opposite signed r_z values, to get a measure of the extent of rotational movement in the flow the difference

$$\max(r_z) - \min(r_z) \tag{9}$$

may be defined as the rotation range. We can now compute the rotation range for each configuration and analyze the behavior in each of the phases considered so far. The results are given in FIG. 16.

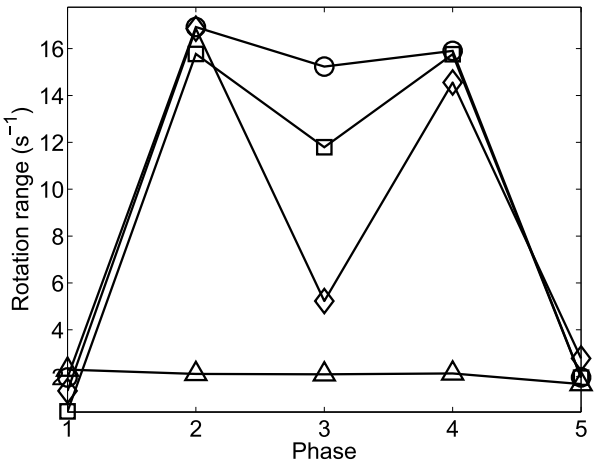

FIG. 16. Rotation range (from minimum to maximum) during the different phases and for each configuration. The following legend is used: circle for the 5/1 configuration, square for the 4/2 configuration, diamond for the 3/3 configuration and triangle for the 6/0 configuration.

Clearly the unidirectional case has a low rotation range during the full length of the experiment. In general, a qualitatively similar behavior is observed in all bidirectional cases with a sort of inverted 'w' shape and with rotation peaking during lane formation and dissolution. Overall, the 5/1 configuration shows the largest rotation range throughout

the experiment, meaning that bidirectional flow with a small minor flow needs continuous turning to avoid collisions with the counter flow. Although all configurations have similar rotation range values during lane formation, the differences become evident once lanes are formed. In phase 3 (full bidirectional flow), rotation range shows a linear relationship with flow-ratio (similar to the order parameter), with the value observed in the balanced case being close to the unidirectional flow. This shows again that the lane formed in the balanced bidirectional case are very efficient, thus requiring only a very limited degree of lateral adjustments. In the 4/2 case, although the rotation range decreases from phase 2 to 3, the reduction is less marked. Finally, it can be noticed that in phase 1 and 5 all the cases have similar values, indicating that, indeed, only unidirectional flow is observed there. In addition, the low rotation range in phase 1 suggests that only little actions are performed to avoid the counter flow and the main process of lane formation actually starts only once pedestrians are very close to each other's. Although the leaders of each group take some measures to adjust their positions and visual interactions are observed, it is only when pedestrians in the back follow their leaders that clear lanes are formed (in phase 2).

TABLE VI. Two-way ANOVA test on the potential combined effect of flow-ratio and phase on the rotation range. Statistics have been conducted at the $p < 0.05$ level, relying on repeated measures (4 runs per configuration).

Factor	ANOVA test results
Flow-ratio	$F(3, 60) = 81.36$, $p < 0.001$
Phase	$F(4, 60) = 139.51$, $p < 0.001$
Interaction	$F(12, 60) = 19.46$, $p < 0.001$

Finally, a two-factors analysis of variance was conducted to test the potential combined effect of flow-ratio and phase on the rotation range. Results reported in TABLE VI clearly show that a significant effect is shown for the flow-ratio factor and the phase factor. In addition, a significant interaction among the two factors (flow-ratio and phase) was found, thus justifying the different slope observed in FIG. 16 for the different flow-ratios.

IV. CONCLUSIONS

Pedestrian bidirectional flow has been studied by designing an experiment in which flow and density have been kept fairly constant and flow-ratio was changed to grasp its influence on lane formation and the efficiency of the flow itself. Experimental conditions were chosen considering previous research (literature) and characteristic situations observed in reality. Aim of the experiment was to study a typical bidirectional flow by collecting a sufficient amount of data using state-of-the-art techniques.

Results show that to understand the phenomena leading to lane formation and to measure the efficiency of each case, 5 different phases need to be distinguished:

- Phase 1: unidirectional free-flow. Both minor and major flow simply keep going straight. Most of pedestrians barely turn in this phase and little anticipating actions are taken to avoid the incoming counter flow.

- Phase 2: lane formation. Pedestrians turn to the left and to the right in a large extent to allow the creation of lanes. The lateral motion is particularly strong in the case of balanced flow. Lanes are formed at the end of this phase.

- Phase 3: full bidirectional flow. Lanes flows separately in a unidirectional manner. The stability is particularly strong in the balanced case, in which each lane can be considered separately, as if a wall would be placed between them. If the difference between the minor and the major flow is large, lanes tend to be more unstable.

- Phase 4: lane dissolution. As the flow becomes partly unidirectional in portions of the surface, lanes are dissolved. Large lateral movements are observed resulting in an high rotation range because pedestrians take advantage of the reduced density while leaving the measurement section.

- Phase 5: unidirectional free-flow. Only unidirectional streams are observed. Again, pedestrians simply keep going straight toward the destination. Rotation is very limited here.

In addition, we showed that statistical quantities are required to analyze pedestrian streams and simple average values are not sufficient to grasp the fundamental characteristics. In this regard, the use of 2D quantities can help understanding some of the behaviors observed and,

in particular, the rotation applied to the velocity vector field has shown being of particular importance. Its applicability with different types of flows (cross, random motion,...) may be a future topic of research.

Finally, our study helped connecting the virtually different conclusions concerning balanced bidirectional flow. We can now say that, once lanes are formed, the balanced bidirectional flow is the most efficient and the capacity can be compared to the one of unidirectional flow. However, the relatively large extent of lateral motion required to create lanes can lead to jam formation when the density increases. This explains why, besides the higher efficiency at low densities, balanced bidirectional flow results in deadlocks earlier compared to low flow-ratio cases at high densities.

Practically speaking, this last conclusion implies that guiding the crowd toward particular directions by helping the lane formation mechanism can improve the capacity of a given corridor, resulting in a lower frequency of deadlock formation.

Future research may focus on more complex cases of bidirectional flows, i.e. high density conditions not considered here or scenarios including a more heterogeneous group of participants composed, for example, of different age groups and different social structures (pairs, families,...). Depending on the situation, the phases derived here may not be observed, but nonetheless we believe that the framework presented in this study can form a basis for the analysis of more complex systems involving pedestrians.

ACKNOWLEDGMENTS

This work was financially supported by JSPS KAKENHI Grant Number 25287026 and the Doctoral Student Special Incentives Program (SEUT RA) of the University of Tokyo. In addition the authors want to thank Daichi Yanagisawa, Andrea Gorrini and Luca Crociani for supervising and preparing the experiment and Takahiro Ezaki for the useful discussion and valuable suggestions.

[1] B. Krausz and C. Bauckhage, Computer Vision and Image Understanding **116**, 307 (2012).

[2] D. Helbing and P. Mukerji, EPJ Data Science **1**, 1 (2012).

[3] A. John, A. Schadschneider, D. Chowdhury, and K. Nishinari, Journal of Theoretical Biology **231**, 279 (2004).

[4] A. Huth and C. Wissel, Journal of Theoretical Biology **156**, 365 (1992).

[5] S. K. You, D. H. Kwon, Y. ik Park, S. M. Kim, M.-H. Chung, and C. K. Kim, Journal of Theoretical Biology **261**, 494 (2009).

[6] T. Vicsek and A. Zafeiris, Physics Reports **517**, 71 (2012).

[7] U. Weidmann, *Transporttechnik der Fussgänger: Transporttechnische Eigenschaften des Fussgängerverkehrs (Literaturauswertung)* (ETH, IVT, 1993).

[8] W. Song, X. Xu, B.-H. Wang, and S. Ni, Physica A: Statistical Mechanics and its Applications **363**, 492 (2006).

[9] D. Yanagisawa, R. Nishi, A. Tomoeda, K. Ohtsuka, A. Kimura, Y. Suma, and K. Nishinari, SICE Journal of Control, Measurement, and System Integration **3**, 395 (2010).

[10] T. Kretz, A. Grünebohm, and M. Schreckenberg, Journal of Statistical Mechanics: Theory and Experiment **2006**, P10014 (2006).

[11] J. Zhang, W. Klingsch, A. Schadschneider, and A. Seyfried, Journal of Statistical Mechanics: Theory and Experiment **2012**, P02002 (2012).

[12] Y. Suma, D. Yanagisawa, and K. Nishinari, Physica A: Statistical Mechanics and its Applications **391**, 248 (2012).

[13] M. Isobe, T. Adachi, and T. Nagatani, Physica A: Statistical Mechanics and its Applications **336**, 638 (2004).

[14] P. Harwood, "Pedestrian microsimulation – a comparative study between the software programs vissim and viswalk," (2013), Master thesis – Chalmers University of Technology.

[15] M. T. Trueblood, in *2006 ITE Annual Meeting and Exhibit Compendium of Technical Papers* (2006).

[16] E. Goubet, J. Katz, and F. Porikli, in *Defense and Security Symposium* (International Society for Optics and Photonics, 2006) pp. 62062C–62062C.

[17] O. Masoud and N. P. Papanikolopoulos, Vehicular Technology, IEEE Transactions on **50**, 1267 (2001).

[18] A. Leykin and R. Hammoud, Machine Vision and Applications **21**, 587 (2010).

[19] C. Dai, Y. Zheng, and X. Li, in *Computer Vision and Pattern Recognition-Workshops, 2005. CVPR Workshops. IEEE Computer Society Conference on* (IEEE, 2005) pp. 13–13.

[20] M. Bertozzi, A. Broggi, A. Fascioli, A. Tibaldi, R. Chapuis, and F. Chausse, in *Intelligent Vehicles Symposium, 2004 IEEE* (IEEE, 2004) pp. 584–589.

[21] I. Karamouzas, B. Skinner, and S. J. Guy, Physical review letters **113**, 238701 (2014).

[22] A. Garcimartín, J. M. Pastor, L. M. Ferrer, J. J. Ramos, C. Martín-Gómez, and I. Zuriguel, Phys. Rev. E **91**, 022808 (2015).

[23] T. Kretz, A. Grünebohm, M. Kaufman, F. Mazur, and M. Schreckenberg, Journal of Statistical Mechanics: Theory and Experiment **2006**, P10001 (2006).

[24] W. H. Lam and C.-y. Cheung, Journal of Transportation Engineering **126**, 343 (2000).

[25] W. H. Lam, J. Y. Lee, and C. Cheung, Transportation **29**, 169 (2002).

[26] W. K. Alhajyaseen and H. Nakamura, {IATSS} Research **34**, 35 (2010).

[27] W. K. Alhajyaseen, H. Nakamura, and M. Asano, Procedia-Social and Behavioral Sciences **16**, 526 (2011).

[28] C. Feliciani and K. Nishinari, Journal of Statistical Mechanics: Theory and Experiment **2015**, P10003 (2015).

[29] C. L. N. Oliveira, A. P. Vieira, D. Helbing, J. S. Andrade, and H. J. Herrmann, Phys. Rev. X **6**, 011003 (2016).

[30] C. Feliciani and K. Nishinari, Physica A: Statistical Mechanics and its Applications **451**, 135 (2016).

[31] G. Flötteröd and G. Lämmel, Transportation research part B: methodological **71**, 194 (2015).

[32] M. Boltes and A. Seyfried, Neurocomputing **100**, 127 (2013).

[33] B. Steffen and A. Seyfried, Physica A: Statistical mechanics and its applications **389**, 1902 (2010).

[34] See Supplemental Material at [URL] for videos of the experiment.

[35] A. Seyfried, B. Steffen, W. Klingsch, and M. Boltes, Journal of Statistical Mechanics: Theory and Experiment **2005**, P10002 (2005).

[36] J. Zhang and A. Seyfried, Physica A: Statistical Mechanics and its Applications **405**, 316 (2014).

[37] M. Saberi, K. Aghabayk, and A. Sobhani, Physica A: Statistical Mechanics and its Applications **434**, 120 (2015).

[38] L. Henderson and D. Lyons, Nature (1972), 10.1038/240353a0.

[39] A. Seyfried, B. Steffen, and T. Lippert, Physica A: Statistical Mechanics and its Applications

368, 232 (2006).

[40] M. Rex and H. Löwen, Physical Review E **75**, 051402 (2007).

[41] S. Nowak and A. Schadschneider, Physical Review E **85**, 066128 (2012).

[42] D. Helbing, A. Johansson, and H. Z. Al-Abideen, Phys. Rev. E **75**, 046109 (2007).

[43] V. G. Ivancevic and D. J. Reid, Nonlinear Dynamics **68**, 285 (2011).